Neutral rare-gas containing charge-transfer molecules in solid matrices. I. HXeCl, HXeBr, HXeI, and HKrCl in Kr and Xe

Mika Pettersson, Jan Lundell, and Markku Räsänen
Laboratory of Physical Chemistry, P.O. Box 55, FIN-00014, University of Helsinki, Finland

(Received 5 December 1994; accepted 17 January 1995)

Ultraviolet-irradiation of hydrogen halide containing rare gas matrices yields the formation of linear centrosymmetric cations of type $(XHX)^+$, (X=Ar, Kr, Xe). Annealing of the irradiated doped solids produces, along with thermoluminescence, extremely strong absorptions in the 1700–1000 cm^{-1} region. Based on isotopic substitution and halogen dependence of these bands, the presence of hydrogen and halogen atom(s) in these species is evident. In the present paper we show the participation of rare gas atom(s) in these new compounds. The evidence is based on studies of the thermally generated species in mixed rare gas matrices. The new species are assigned as neutral charge-transfer molecules HX^+Y^- (Y=halogen), and their vibrational spectra are discussed and compared with those calculated with *ab initio* methods. This is the first time *hydrogen and a rare gas atom has been found to make a chemical bond in a neutral stable compound*. The highest level *ab initio* calculations on the existence of compounds of type HXY corroborate the experimental observations. The mechanism responsible for the formation of these species is also discussed. © *1995 American Institute of Physics.*

INTRODUCTION

The rare gases make up about 1% of the earth's atmosphere, the major component being Ar. Their inertness toward chemical bond formation has been attributed to the ''stable octet'' outer electronic structure, the criterion valid especially for the lighter group 18 elements. No stable neutral compounds of He, Ne, or Ar are known, and their computationally predicted chemical compounds are thoroughly discussed in the review article by Frenking and Cremer.[1] Extensive search for rare gas compounds started in 1962 when Bartlett[2] prepared for the first time the Xe-compound $Xe^+[PtF_6]^-$. The known chemistry of Xe today comprises several compounds, fluorine and/or oxygen atoms being typically involved in these compounds. The chemistry of Kr is confined to the difluoride and its derivatives.[3] KrF_2 is a linear molecule [the bond distance Kr–F being 1.875 Å (Ref. 4)], and it decomposes slowly at room temperature.

Matrix photogeneration of linear triatomic cations $(XHX)^+$ (X=Ar, Kr or Xe) and anions $(YHY)^-$ (Y=Cl, Br or I) is presently rather well understood.[5–7] Spectroscopically these isoelectronic pairs show great similarities; their structure is $D_{\infty h}$, and the large anharmonicity of the bonds leads to unexpectedly strong combination absorptions in the 700–1300 cm^{-1} spectral region.[8,9] These $\nu_3 + n\nu_1$ progressions are visible in the mid-infrared region up to n value of 5. The mechanism responsible for the formation of the rare gas cationic species involves generation of hydrogen atoms and an electronegative center (for instance a halogen atom) in the matrix. Further irradiation of the matrix at ultraviolet wavelengths results in charge separation in the Rg–electronegative center pair, and a delocalized hole is generated photolytically. The photophysics connected with these two-step processes is well understood on the basis of the pioneering studies of Fajardo and Apkarian.[10–12] In the case of photodissociation of hydrogen halides in rare gas matrices, one of the stabilization sites of the positive charge is in the form of the centrosymmetric $(XHX)^+$ cations, while the electron is deeply trapped in the halogen atom. Other trapping sites besides $(XHX)^+$ have not yet been experimentally characterized. The trapped holes can be thermally mobilized by increasing the matrix temperature to 30–50 K, and strong thermoluminescence is connected with this process.[5,6,12] The most probable process occurring to the mobilized holes in the matrix is neutralization, and a large energy release by either nonradiative or radiative processes. The threshold temperature for thermoluminescence in Xe is typically 40 K.

Annealing of the system obtained from photodissociation of HY (Y=halogen) yields a number of extremely intense absorptions in the 1000–1700 cm^{-1} region.[7] Figure 1 displays the infrared spectra of HI in Xe after different treatments pointing out the enormous intensity of the thermally activated species dealt with in this paper. Based on original measurements of photodissociation of hydrogen halides in different rare gases it has been possible to deduce only two of the atoms involved in these compounds. First, hydrogen is involved, the deuterium shift being typically about 1.34, displaying a strongly anharmonic potential. Additionally, the precursor dependence shows that also halogen atom(s) is involved. Due to the broadness of these bands it is quite difficult to make any detailed conclusions about the number of halogen atoms involved. Further, these absorptions also suggest the participation of rare gas atoms in these species. The characteristic thermal absorptions are experimentally obtainable in Xe matrices while photolyzing precursors containing Cl, Br or I atoms. However, in Kr matrices the thermal product can be detected only after photolysis of HCl. It must be noted also that we have not yet attempted to photolyze HF in rare gas matrices. A tentative assignment of the thermal products has been given by Kunttu and Seetula.[7] This proposed assignment is based on the early experiment of Evans and Lo[13,14] on the symmetrical and unsymmetrical $(YHY)^-$-anions (Y=halogen), strongly perturbed by the

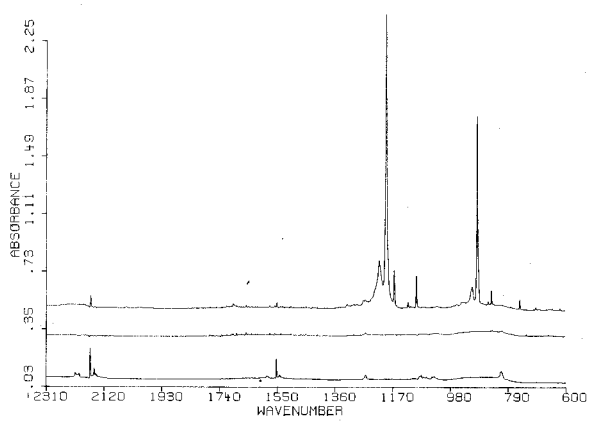

FIG. 1. Photolysis of HI/DI in Xe (M/A∼200). The lowest trace shows the situation after deposition at 50 K (recorded at 15 K), indicating almost equal amounts of H- and D-precursors. The middle trace is after Hg-arc irradiation, showing complete photodissociation of the precursor. Annealing the photolyzed matrix at 45 K yields the uppermost spectrum with basically two extremely intense bands. It is to be noted that all of the spectra shown are drawn in the same absorbance scale.

nearest-neighbor cation. Also the assignment of the thermal products as HXY^+ cations was discussed.[7]

Quite interestingly, Last and George[15] in their computational studies for impurity centers in rare gases predicted the existence of an ionic molecule $(HXe)^+Cl^-$. The computation was based on the semiempirical diatomics-in-ionic-systems (DIIS) method. According to the calculation, the ground state $(HXe)^+Cl^-$ molecule is linear and separated from the van der Waals complex HCl···Xe by a barrier of 0.41 eV. The DIIS calculation suggests two strong bonds for this system, the $(H–Xe)^+$ and $Xe^+–Cl^-$, the former subspecies being isoelectronic with HI. Also, the calculations suggest quite extensive charge separation, leading to a very large dipole moment (15 D) for this molecule. From the experimental point of view it is of interest also to note that the DIIS results for the first excited state suggest a geometry of $(XeH)^+Cl^-$. This leads to a considerable lowering of the barrier between the ionic molecule and its HCl···Xe van der Waals complex in the electronically excited state.

COMPUTATIONAL DETAILS

All calculations were performed within the framework of the GAUSSIAN 92 (Ref. 16) package of computer codes. Electron correlation was considered via Møller–Plesset perturbation theory[17,18] to the second order, including all electrons. The harmonic frequencies were calculated analytically at the UMP2 level of theory, and the high level UCCSD (Refs. 19–22) calculations were used to generate the HArF potential energy surface.

The applied basis sets display three different ways of describing the electronic structure of the atoms of concern. Effective core potentials (ECP) were introduced in the LANL1DZ presentation by Wadt and Hay,[23–25] and the relativistic presentation by Christiansen.[26–28] Generally the Cl and Ar atom basis sets are described with an explicit 7 or 8 electrons valence shell, respectively, while the chemically less active core electrons are pictured with effective potentials. For the heavier rare gas atoms (Kr and Xe) and halogen atoms (Br and I) the accuracy of calculations was improved in the ECP approach by inclusion of the underlying d-orbital in the valence space, resulting in a total of 18 or 17 valence electrons, respectively. Furthermore, for Ar and Cl the balanced atomic basis sets developed by Wallace *et al.*[29] (WBP) were used within the Christiansen ECP approach.

The all-electron approaches are based on the standard, split-valence type, double-ζ basis set augmented with a d-polarization function (6-31G*) (Refs. 30–32) for Ar, F, and Cl, and the Huzinaga basis sets[33] for heavier atoms. For Cl the Huzinaga $11s8p$ basis set was used contracted as (533/5111). In the case of Kr and Br the $13s10p4d$ basis sets were used contracted as (4333/433/4). For Xe and I the basis set notation is $16s13p7d$ with a contraction of (43333/4333/43).

For the hydrogen basis the standard, split valence type, double-ζ basis sets, added with a single p-polarization function ($3s1s1p$ and $3s1s1s1p$) were chosen. However, the large $7s2p1d$ (contracted as 211111/11/1) by Rosmus,[34] and the modified $3s1s$ basis ($3s1s1s1p1p$) by Latajka and Scheiner,[35] denoted as $+VP^S(2p)^S$, were also tested.

All calculations were carried out on CRAY X-MP EA/464, SGI Power Onyx, and Convex C3840 supercomputers at the Center for Scientific Computing (Espoo, Finland).

EXPERIMENT

HBr was synthesized from tetrahydronaphtalene and bromine[36] and was purified by low temperature distillation. HCl (Matheson) of technical purity was used without further purification. Xenon of 99.997% and krypton of 99.99% purity (Messer Griesheim) were used with their original purities. HBr was stored in a blackened glass bulb in order to reduce the decomposition of the gas. Gas mixtures were prepared in a glass manifold using standard manometric procedures. Premixed gas was sprayed through a 1/16 in. stainless steel capillary onto a CsI substrate. Substrate temperature of 30 K was used in most experiments. Typically ∼4 mmol of the gas mixture was deposited at the rate of 2.7 mmol/h. After deposition the solids were slowly cooled to 15 K. A closed cycle helium refrigerator (Displex, DE-202A) was used for cooling. The matrix was warmed with a resistive heater and the temperature was measured with a silicon diode (accuracy 0.1 K) attached on the frame of the cold substrate. An excimer laser was used as the photolysis source. The laser (Estonian Academy of Sciences, ELI-76) was operated at 193 nm (ArF), and the pulse energies used were typically 5–20 mJ. The infrared spectra were recorded with a Nicolet 60SX Fourier transform spectrometer capable to a resolution of 0.25 cm^{-1}, coadding typically 200 scans.

RESULTS AND DISCUSSION

193 nm irradiation of the ternary HCl/Xe/Kr and HBr/Xe/Kr solids at 15 K produces the ionic species, identified previously as Xe_2H^+, Kr_2H^+, Cl_2H^-, and Br_2H^-. The structure of all these species is linear centrosymmetric.[5,6,8,9,37–42] Annealing of the extensively irradiated solids near 40 K causes the appearance of strong IR-absorptions in the 800–

TABLE I. Thermally induced peaks in different H(D)Y/X matrices (Y=Cl, Br, I, X=Xe, Kr). The main absorptions are underlined.

Matrix	Observed wave numbers
HCl/Xe	1648.7, 1648 (s), 1646 (sh)[a]
DCl/Xe	1197.8, 1197.3 (m), 1196 (sh)
HBr/Xe	1504 (vs), 1500 (sh), 1519, 1487 (sidebands), 489 (w), 486 (w), 965 (overtone)[b]
DBr/Xe	1100 (s)
HI/Xe	1193 (vs), 1187 (sh), 1215 (sideband), 450 (w), 447 (w)
DI/Xe	893 (vs), 889 (sh), 909 (sideband)
HCl/Kr	1476 (vs), 1495, 1458 (sidebands), 544 (w), 1070 (overtone)[b]
DCl/Kr	1106 (s), 1126 (sideband)

[a]The 597 cm^{-1} peak from Ref. 7 could not be reproduced.
[b]This work, other values are taken from Ref. 7.

1700 cm^{-1} region (cf. Fig. 1). It is also to be noted that careful kinetic measurements show that the disappearance of the centrosymmetric cations is not connected with the formation of the thermally generated species.[7]

Table I lists the observed thermally induced peaks in different H(D)Y/X systems in various rare gas matrices (Y =Cl, Br, I; X=Xe, Kr), respectively. The data are adapted from Ref. 7. Importantly, HCl is the only hydrogen halide producing the thermally induced peaks both in Kr and Xe (experiments with HF precursor are underway in our laboratory). The large difference (173 cm^{-1}) between the wave numbers of the HCl/Xe (1649 cm^{-1}) and HCl/Kr (1476 cm^{-1}) annealing products would indicate that the peaks belong to different species rather than to the same species in different hosts. In order to verify which one of the cases is correct we have made photodissociation and annealing experiments with ternary HCl/Kr/Xe mixtures.

Figure 2 represents the spectrum obtained from a HCl:Xe:Kr=1:5:500 sample which has been extensively irradiated by ArF-excimer laser and thereafter annealed to 50 K. There are two characteristic peaks in the spectrum in the region of 1800–1400 cm^{-1}, which appear during the thermal treatment of the matrix. One of them (at 1475.7 cm^{-1}) corresponds to the HCl/Kr thermally induced peak and the other

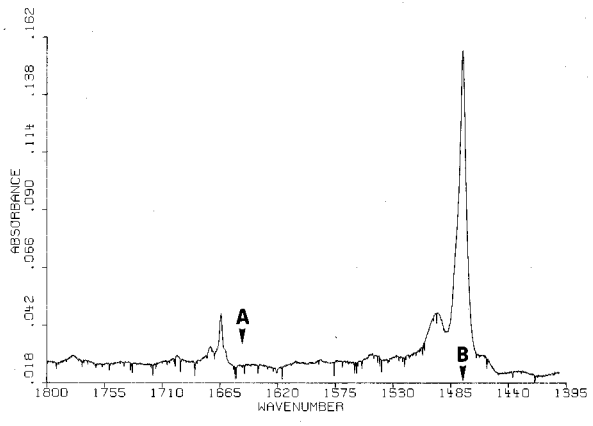

FIG. 2. Thermally induced spectral bands of a ternary HCl:Xe:Kr (1:5:500) mixture. The arrows indicate the positions of the thermal bands obtained in pure Xe (a) or Kr (b) matrices after photolysis of HCl.

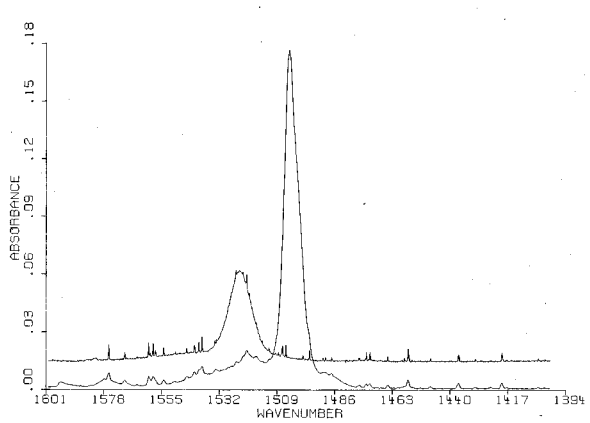

FIG. 3. Thermally induced absorptions of photolyzed HBr/Xe/Kr matrices. A Xe concentration of 5% yields the band at higher wave numbers and the concentration of Xe is 95% for the lower wave number spectrum. The spectra are drawn on the same scale and in these experiments the amount of mixture deposited was the same.

one (at 1664.4 cm^{-1}) corresponds to the HCl/Xe thermally induced peak, shifted 15 cm^{-1} to higher wave numbers from its value in pure Xe. The lower wave number peak of the thermally generated species of HCl/Kr (544 cm^{-1}) is also observed in the mixed matrices but the corresponding peak of HCl/Xe is too weak to be observed. This simple experiment indicates that the thermally induced peaks belong to two different species. Moreover, it suggests that each of the species involved contains at least one rare gas atom.

Similar experiment was made with HBr and Xe doped krypton (HBr:Xe:Kr=1:5:500). As reported previously,[7] the thermal product after photolysis of HBr doped matrices was obtained only in Xe, even though the trapped hole was present in Xe and Kr, as indicated by the $(XHX)^+$ (X=Xe or Kr) absorptions. In accordance with this, in the present mixed matrix case only one thermally induced peak was observed, located close to the value of the thermally induced absorption in the pure HBr/Xe system (at 1504 cm^{-1}). The wave number of the peak is 1524 cm^{-1}, which corresponds to a shift of +20 cm^{-1} compared to its value in pure xenon. Figure 3 shows the spectrum of the thermal product in two different Xe/Kr matrices, and we may note that the intensity of the thermal product corresponds qualitatively to the concentration of Xe in the mixture and that the only species forming is similar to that found in the case of photolysis of HBr in pure Xe. Additionally, the wave number of the thermally induced species in mixed matrices approaches at higher Xe concentrations that obtained in pure Xe.

Based on deuterium shift and halogen dependence the thermally induced species contain one hydrogen atom and at least one halogen atom[7] and on the basis of the present experiments at least one rare gas atom. We have also good reasons to assume that the strong thermally generated absorptions in the HI/Xe system belong to a similar species containing hydrogen, iodine, and Xe. Assuming the simplest possible formula for the species leaves us with two candidates, a charged or a neutral HXY, where Y may be Cl, Br or I with X=Xe and Y is only Cl in the case of X=Kr. The cases of Y being F will be discussed below.

TABLE II. Observed wave numbers for hydrogen stretching in Kr and Xe matrices for some anions and neutral species.

Species	ν(Kr)/cm^{-1}	ν(Xe)/cm^{-1}	$\Delta\nu$/cm^{-1}	$\Delta\nu/\nu$(Kr)
HI_2^-	647[a]	581[a]	66	10.2%
HBr_2^-	687[a]	646[a]	41	6.0%
HCl_2^-	663[a]	644[a]	19	2.9%
HBr	2552[b]	2532[b]	20	0.8%
HCl	2873[b]	2853[b]	20	0.7%
HBr/Xe thermally induced peak	1524[c]	1504[c]	20	1.3%
HCl/Xe thermally induced peak	1664[c]	1649[c]	15	0.9%

[a]From Ref. 6.
[b]From Ref. 7.
[c]This work.

Our recent *ab initio* studies[43] on $ArHY^+$, $KrHY^+$, and $XeHY^+$ (Y=Cl, Br, I) suggest both linear and bent ground state structures for these ions. According to the MP2/ECP/+$VP^S(2p)^S$ computational approach the bent structures appear to be the lowest-energy species in the cases of $KrHCl^+$, $XeHCl^+$, and $XeHBr^+$, while the lowest-energy structure for the others is linear. The calculated spectra of the linear species resemble the spectra of the thermally induced species in matrices. This causes a controversy for assigning the products as cations on the basis of the computed spectra, since it would require that in HCl/Kr, HCl/Xe, and HBr/Xe only higher energy species could be generated, while in HBr/Xe and HI/Xe only lower energy species are obtainable. There are also quite large discrepancies between the calculated and observed spectra. For example, for $KrHCl^+$ the calculated wave number for the ω_3 fundamental is more than 500 cm^{-1} higher than the observed wave number of the thermally generated species in Kr matrix. Also according to the calculations[43] the species $KrHBr^+$ and $KrHI^+$ should be stable but they have not been observed in matrices. Additionally, the energetics for the possible formation of XHY^+ species deserves some discussion. For example, the calculated lowest energy dissociation asymptote of $XeHCl^+$ is given as Xe^++HCl and it is predicted to lie 0.067 eV above the energy of the linear $XeHCl^+$. However, dissociation of the cation in a xenon cage would immediately lead to the formation of a Xe_2^+ or a Xe_3^+ rather than Xe^+. Taking into account the dissociation energy of Xe_2^+ of 1.08 eV,[44] the actual dissociation asymptote of $XeHCl^+$ is ~1 eV lower in energy than the linear form of the cation. This makes the existence of the $XeHCl^+$ species in xenon environment rather improbable.

The vibrational spectra of ions shift more than the spectra of neutral species in going from one rare gas environment to the other. In Table II we present the vibrational wave numbers for some ions and neutral molecules in xenon and krypton matrices. Included are also for comparison the wave numbers of the thermally induced peaks of HCl/Xe and HBr/Xe mixtures. The relative vibrational shifts of the thermally induced peaks are between those of ions and hydrogen halides and the shifts support the assignment of the thermal products as neutral species, possessing a relatively strong dipole.

At first, it would seem impossible to form a bound ground state molecule out of a closed shell rare gas atom with a hydrogen and a halogen atom. However, encouraged by the results of Last and George[15] on HXe^+Cl^- we have carried out *ab initio* calculations at different levels. Indeed, the *bound ground state structure of neutral HXY molecules is reproducible*. Table III shows the calculated properties of the HXY (X=Ar, Kr, Xe; Y=F, Cl, Br, I) species. All of the optimized structures are linear. In the optimizations it was of crucial importance to start with bond lengths which were near the optimized values because too large values led the system into the repulsive part of the surface. The calculated parameters change somewhat when different basis sets are used, but qualitatively the picture stays the same. One impor-

TABLE III. *Ab initio* calculated properties of neutral HXY species at different levels.

	Method	R_{Rg-H} (Å)	R_{Rg-Hal} (Å)	q_H[a]	q_{Rg}[a]	q_{Hal}[a]	μ(D)	E(a.u.)
HXeF	UMP2/43333/4333/43 (Xe)/6-31G** (F)/ 6-311G**(H)	1.6687	2.1393	−0.073	+0.779	−0.707	6.1	−7 326.809 579 4
HXeCl	UMP2/LANL1DZ	1.8085	2.7844	−0.041	+0.693	−0.652	8.9	−30.388 300 3
	UMP2/ECP (Xe)/WBP (Cl)/6-311G**(H)	1.8098	2.8226	−0.016	+0.520	−0.504	6.9	−141.138 256 7
	UMP2/43333/4333/43 (Xe)/533/5111 (Cl)/ 6-311G**(H)	1.6736	2.8519	+0.040	+0.664	−0.704	10.7	−7 686.661 758 6
HXeBr	UMP2/LANL1DZ	1.8690	2.9775	−0.036	+0.626	−0.590	8.8	−28.609 107 7
	UMP2/ECP (Xe,Br)/6-311G**(H)	1.8490	3.0130	−0.004	+0.464	−0.460	6.9	−279.504 569
	UMP/2/43333/4333/43(Xe)/4333/433/4(Br)/ 6-311G**(H)	1.7801	2.9780	−0.011	+0.528	−0.518	7.7	−9 797.318 977 1
HXeI	UMP2/LANL1DZ	2.0426	3.2391	−0.024	+0.512	−0.487	7.9	−26.836 799 6
	UMP2/ECP(Xe,I)/+$VP^S(2p)^S$	1.9157	3.2594	+0.002	+0.384	−0.386	6.3	−235.871 557 4
	UMP2/43333/4333/43 (Xe,I)/6-311G**(H)	1.8140	3.2216	+0.002	+0.477	−0.478	7.9	−14 140.111 731
HKrF	UMP2/4333/433/4 (Kr)/6-31G**(F)/6-311G**(H)	1.5256	2.0383	+0.026	+0.627	−0.652	6.2	−2 849.494 813 1
HKrCl	UMP2/ECP (Kr)/WBP (Cl)/6-311G**(H)	1.7348	2.6629	+0.040	+0.365	−0.405	5.5	−192.066 222 4
	UMP2/4333/433/4 (Kr)/533/5111 (Cl)/6-311G**(H)	1.5337	2.6866	+0.135	+0.530	−0.665	10.2	−3 209.338 929 5
HArF	UMP2/6-31G**	1.3928	1.9409	+0.045	+0.526	−0.571	5.1	−626.857 992 9
HArCl	UMP2/6-31G**	1.3939	2.5013	+0.123	+0.450	−0.573	7.8	−986.902 985 4

[a]Partial atomic charges based on Mulliken population analysis.

tant result during the optimizations appeared; neither HKrBr nor HKrI could be optimized at any of the levels used in the calculations. This suggests that such molecules do not exist. This is in accordance also with the experiments, because in HBr doped krypton or in HI doped krypton no thermally induced peaks have been observed. Knowing these facts no attempts to optimize HArBr or HArI were made.

Inspection of the data given in Table III shows that these species are charge-transfer molecules. In all of them the rare gas has donated electron density to the halogen atom. As a consequence of a charge transfer the properties of the rare gas atom should approach those of the corresponding isoelectronic halogen atom. Also, at the extreme of charge separation the system looks like a HX^+-cation (which are strongly bound),[34,45,46] connected to a Y^--anion. The calculations indicate that stretching the X–Y coordinate from its equilibrium value yields HX^+ and Y^- as the dissociation asymptote. The existence of HXY charge-transfer molecules can be rationalized in terms of HX^+ and X^+Y^- pair potentials which are both strongly bound.[34,47] As an example the HXe^+ and Xe^+Cl^- potentials are displayed in Fig. 4. The difference in energy between ionic Xe^+Cl^- and neutral XeCl at Xe^+Cl^- equilibrium structure is given as

$$\Delta E(R=R_{e,\text{ionic}}) = \text{IP(Xe)} - \text{EA(Cl)} - D_e(\text{Xe}^+\text{Cl}^-) - E(\text{XeCl}, R=R_{e,\text{ionic}}). \quad (1)$$

Ignoring the last term as small compared with the other values gives

$$\Delta E = \text{IP(Xe)} - \text{EA(Cl)} - D_e(\text{Xe}^+\text{Cl}^-). \quad (2)$$

Inserting the following values: IP (Xe)=12.130 eV,[50] EA (Cl)=3.613 eV,[50] D_e (Xe^+Cl^-)=4.53 eV (Ref. 51) gives the energy difference the value of 3.99 eV. Interaction of a hydrogen atom with Xe^+Cl^- yields $(Xe–H)^+$-type of bond, which lowers the energy of the molecule by the value, which maximally could be the dissociation energy of XeH^+[$D_0(XeH^+)$=3.90 eV (Ref. 34)]. Assuming that the H–Xe bond length in HXeCl charge-transfer molecule is only slightly larger than the equilibrium value of the HXe^+ bond length we are led to a situation where the HXeCl molecule could be lower in energy than a repulsive H+Xe+Cl configuration. The reason for this is the shape of the neutral H–Xe potential which raises the energy of the repulsive configuration when Xe–H separation approaches the equilibrium value of $(XeH)^+$. These considerations suggest that when H, Xe, and Cl atoms are forced to approach each other, the charge-transfer molecule becomes a minimum energy configuration. In order to check the idea we have calculated the minimum energy dissociation path for HXeCl by stretching the H–Xe coordinate and optimizing the Xe–Cl coordinate at each H–Xe value. The results are shown in Fig. 5. It can be seen that at the minimum energy configuration ionic HXeCl is lower in energy than the repulsive triplet state. At larger values for H–Xe and Xe–Cl bond distances the triplet state becomes lower in energy. Thus, once formed, the HXeCl charge-transfer molecule is stable at a local minimum configuration. The possible stabilizing consequences of solvation in the solid environment will be discussed later.

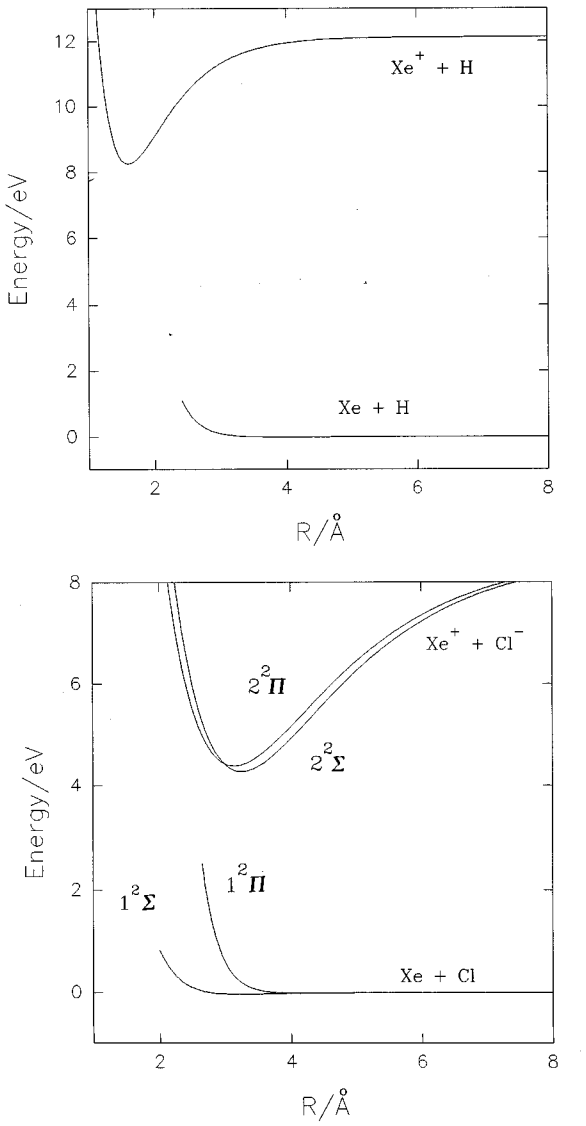

FIG. 4. Energetics of different diatomic combinations for HXeCl. The energy of the XeH^+ surface in the upper panel is scaled to 12.13 eV at infinite separation (ionization energy of Xe). The data for construction of the graphs is taken from Ref. 47 for Xe^+Cl^-, from Ref. 48 for Xe+Cl, from Ref. 49 for Xe+H, and from Refs. 34 and 45 for XeH^+.

The partial charge transfer makes all the molecules studied quite strong dipoles. The computed partial charge of hydrogen is nearly zero in all of the molecules with the exception of HKrCl and HArCl in which cases the hydrogen carries a significant positive charge. Charge transfer from a rare gas atom to a halogen makes it possible for a hydrogen to form a relatively strong bond with the rare gas atom. The bond length between hydrogen and xenon is increased when the halogen changes from the most electronegative fluorine to the least electronegative iodine. Simultaneously, the amount of charge transfer between Xe and halogen is reduced. Krypton, which has higher ionization potential than xenon can form hydrogen containing triatomic compounds only with the most electronegative halogens, fluorine, and chlorine. According to our calculations also argon should form compounds with fluorine and chlorine. Computations

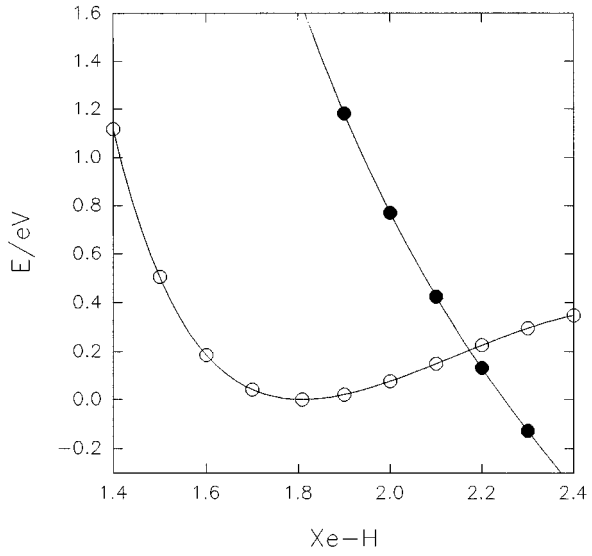

FIG. 5. The UMP2/LANL1DZ calculated potential energy surfaces for different configurations of HXeCl. The open circles indicate the singlet surface with respect to the H–Xe bond length. At all H–Xe values the Xe–Cl bond distance was optimized. The filled circles show the triplet energetics calculated at the corresponding singlet geometries.

on neon compounds have not been attempted.

The computed hydrogen-rare-gas bond length is quite sensitive to the basis set used. For example in HXeI it reduces 0.2286 Å in going from LANL1DZ basis set to the all-electron treatment. The calculated hydrogen-rare-gas bond lengths may be compared with the slightly shorter experimental values of diatomic hydrogen-rare-gas cations, which are 1.6028 Å, 1.4212 Å, and 1.2804 Å for XeH^+, KrH^+, and ArH^+, respectively.[45,46] These numbers are also in agreement with the idea of the HXY species being at the extreme of charge transfer of type HX^+Y^-, as discussed above.

The calculated harmonic wave numbers for HXY species are presented in Table IV. For comparison, the observed wave numbers of the thermally induced species are also included. At all levels the bending wave numbers correspond quite well to the observed values, but the hydrogen stretching wave number is strongly dependent on the computational level used. However, the correspondence between the calculated and observed wave numbers is satisfactory at the most extensive, all electron treatment of the problem. Additionally, the calculated intensities are qualitatively in accordance with the experiments, where extremely high intensities are found for the higher wave number peaks (hydrogen stretching), and low intensities for the lower wave number peaks (bending). The intensity of the hydrogen stretching is highest for HXeI in the series of the HXY species, in qualitative accordance with experimental observations (the concentration of the thermally generated species is not known). Also, the computed intensity of bending is highest for HKrCl, which seems to be the case experimentally as well.

The calculations not only support the assignment of the observed thermally induced peaks in matrices as neutral HXY species, but they also predict the existence of the previously unobserved species HXeF, HKrF, HArF, and HArCl. The experimental work in order to observe these species is underway in our laboratory.

TABLE IV. *Ab initio* calculated harmonic wave numbers of neutral HXY species at different levels. Numbers in parentheses are intensities (km/mol).

	Method	ν_{Rg-Hal}	$\delta_{H-Rg-Hal}$	ν_{H-Rg}
HXeF	UMP2/43333/4333/43 (Xe) 6-31G**(F)/ 6-311G**(H)	495.7(121)	738.6 (14)	2059.7 (649)
HXeCl	UMP2/LANL1DZ	262.0 (26)	503.4 (5)	1246.2 (3133)
	UMP2/ECP (Xe)/WBP (Cl)/6-311G**(H)	272.6 (2)	510.0 (0.4)	1459.5 (4034)
	UMP2/43333/4333/43 (Xe)/533/5111 (Cl)/ 6-311G**(H)	251.3 (78)	545.5 (3.7)	1887.1 (2136)
	experimental			1649
HXeBr	UMP2/LANL1DZ	177.7 (2)	455.1 (3)	1008.4 (4177)
	UMP2/ECP (Xe,Br)/6-311G**(H)	181.7(0.2)	461.0 (0)	1247.0 (5570)
	UMP2/43333/4333/43 (Xe)/4333/433/4 (Br)/ 6-311G**(H)	181.0 (2)	506.0 (0)	1347.8 (4742)
	experimental		489 486 (7)[a]	1504 (1000)[a]
HXeI	UMP2/LANL1DZ	101.7 (89)	355.7 (3)	536.0 (3885)
	UMP2/ECP (Xe,I)/+$VP^S(2p)^S$	131.7 (23)	404.5 (0.1)	899.8 (7595)
	UMP2/43333/4333/43 (Xe,I)/6-311G**(H)	140.6 (0)	461.8 (0.6)	1155.7 (7030)
	experimental		450 447 (5)[a]	1193 (1000)[a]
HKrF	UMP2/4333/433/4 (Kr)/6-31G**(F)/ 6-311G**(H)	535.6(105)	782.7 (0)	1973.7 (1563)
HKrCl	UMP2/ECP (Kr)/WBP (Cl)/6-311G**(H)	235.0 (83)	492.6 (1.6)	977.4 (4581)
	UMP2/4333/433/4 (Kr)/533/5111 (Cl)/ 6-311 G**(H)	272.8 (93)	566.9 (24)	1692.1 (5168)
	experimental		544 (23)[a]	1476 (1000)[a]
HArF	UMP2/6-31G**	521.4(121)	794.7 (1.4)	1723.8 (2950)
HArCl	UMP2/6-31G**	299.2(211)	612.4 (19)	1420.4 (8395)

[a]Experimental relative intensities based on integrated peak areas. Higher intensity has been given a value of 1000.

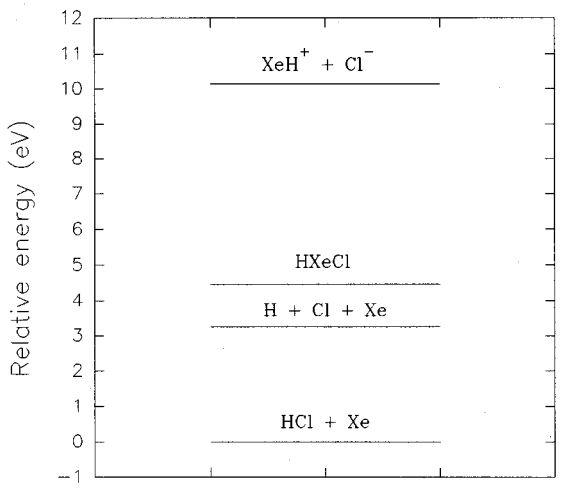

FIG. 6. The UMP2/LANL1DZ-calculated energies of the different precursor combinations involved in the formation of HXeCl. The energies of the fragments are calculated at infinite separation.

MECHANISTIC ASPECTS

The HXY species are metastable with respect to dissociation into hydrogen halides and rare gas atoms, and also with respect to dissociation into neutral atoms, as discussed previously. In order to get a qualitative insight of the formation route, we have calculated the energetics of the possible precursors $[(HXe^+ + Cl^-)$, $(HCl + Xe)$, and $(H + Xe + Cl)]$ of HXeCl at the UMP2/LANL1DZ-level. The results are presented in Fig. 6. It can be seen that HXeCl is higher in energy than the infinitely separated atoms. However, in a solid rare gas environment the energy of a strong dipole HXeCl is lowered due to solvation in the dielectric medium. This is probably a very important effect when considering the stability of HXY-charge-transfer molecules. As a numerical example we can take the difference of the $B \leftrightarrow X$ transition of XeCl in gas phase and in solid Xe, yielding a value of 0.53 eV attributable to solvation of Xe^+Cl^- in Xe.[10] Knowing that HXeCl is formed by annealing the matrix it seems clear, that it cannot be formed from neutral atoms. Warming up the matrix should drive the reaction into the direction in which lower energy species are formed. Also considering the repulsive nature of neutral H–Xe and Xe–Cl potentials leaves us with the conclusion, that ions must take part in the formation process of HXeCl and related species.

One possible formation route could be the following: After extensive irradiation of a hydrogen-halide doped rare-gas matrix there are several neutral and ionic species present in the matrix, including halogen ions, hydrogen atoms and trapped Rg_n^+-centers.[12] The range of migration of hydrogen atom from the site of photodissociation is not known but some of the hydrogen atoms may be located near the halogen ions, which are surrounded by rare-gas atoms. The charge-transfer excitation may provide the hole with enough kinetic energy to escape the precursor site,

$$Y^- \cdots X \cdots H \cdots (X)_m \cdots X_n^+$$

or

$$Y^- \cdots (X_m) \cdots (XHX)^+. \tag{3}$$

Annealing the matrix would then result in mobilization of the trapped holes and subsequent neutralization of charges. Consequently, a reaction of a thermally mobilized hole (MH) with a $Y^- \cdots X \cdots H$-center could result in the formation of a high energy neutral YXH-species,

$$Y^- \cdots X \cdots H + MH \rightarrow YXH. \tag{4}$$

The formation temperature of HXY-species correlates well with the temperature in which thermoluminescence from the matrix is detected, resulting from mobile holes neutralizing negative ions.[12] Another reaction which could produce HXY is a reaction of X^+Y^- with a hydrogen atom

$$X^+Y^- + H \rightarrow HXY. \tag{5}$$

Fajardo and Apkarian[10] have demonstrated that Xe^+Cl^- in Xe forms readily the triatomic configuration $Xe_2^+Cl^-$, which then relaxes radiatively,

$$Xe^+Cl^- + Xe \rightarrow Xe_2^+Cl^- \xrightarrow{573\ \text{nm}} 2Xe + Cl. \tag{6}$$

X^+Y^- is formed by UV-irradiation and it is possible that also HXY is formed simultaneously. However, this reaction cannot produce HXY in significant amounts because irradiation also destroys it.[7] One more possible formation route for HXY would be the reaction of a proton with a XY^- center,

$$H^+ + Y^-X \rightarrow HXY. \tag{7}$$

This mechanism has to be rejected because in the rare gas matrices proton is stabilized in the form of $(XHX)^+$, and the disappearance of these cationic centers is not correlated with the formation of the HXY charge-transfer molecules.

Because the HXY species are metastable with respect to dissociation to atoms or HY and X, it is important to investigate the potential barrier heights in order to find out how stable the species are. It is known from annealing experiments, that in xenon and krypton matrices HXeCl, HXeBr, HXeI, and HKrCl are stable up to the sublimation temperature of the solid. We have scanned the potential energy surface of HArF using coupled cluster (UCCSD) approach. We have chosen UCCSD, because it should give the dissociation asymptote correctly,[52] and HArF, because it is the smallest HXY system allowing high level calculations. The potential energy surface of the linear molecule is presented in Fig. 7. In order to find the height of the potential barrier we have calculated the minimum energy path to dissociation by stretching the Ar–H bond and optimizing the Ar–F bond length at each fixed value of Ar–H. The results are given in Fig. 8 indicating a barrier of ~0.18 eV. We have also calculated a few points of the minimum energy path with respect to the bending coordinate of HArF. The results indicate the barrier height of at least 0.48 eV, which is larger than the barrier height with respect to stretching of the linear configuration. The highly correlated calculations of barrier heights for other HXY species is beyond the scope of this paper.

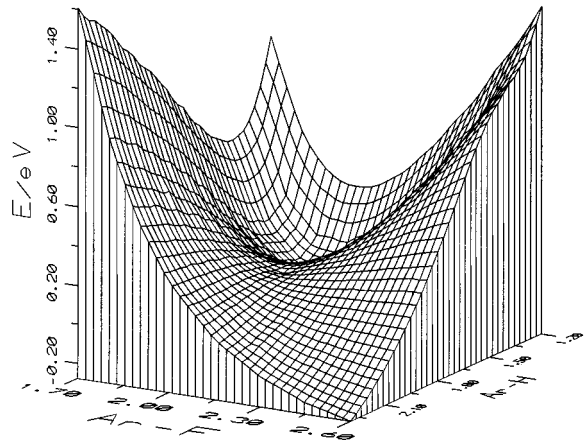

FIG. 7. The potential energy surface of HArF, calculated at the UCCSD=Full/6-31G**-level. A total of 108 points were calculated for construction of the surface.

The calculated values indicate, that it should be possible to stabilize HArF in the matrix environment. Solvation of a strong dipole in the dielectric host should also stabilize HArF significantly with respect to dissociation asymptote, as discussed previously. Also, once HArF is formed, the surrounding rare gas atoms may prevent its dissociation via the cage effect. All these considerations make HArF a potential candidate for a first neutral argon compound.

Given a dissociation barrier height of 0.18 eV for HArF it is expected, that krypton and xenon compounds are even more stable since the heavier rare gas atoms have lower ionization potentials and they are more polarizable than Ar. Lower ionization potential leads to more efficient charge separation between X and Y which in turn strengthens the H–X bond. Finally, if the potential barrier were very low it would lead to tunneling to the repulsive surface. However, tunneling effects are not observed (all the species are stable at 15 K), which indicates significant height for the barrier between the bound and repulsive configurations. Theoretical, computational, and experimental work considering the new rare gas compounds is strongly encouraged.

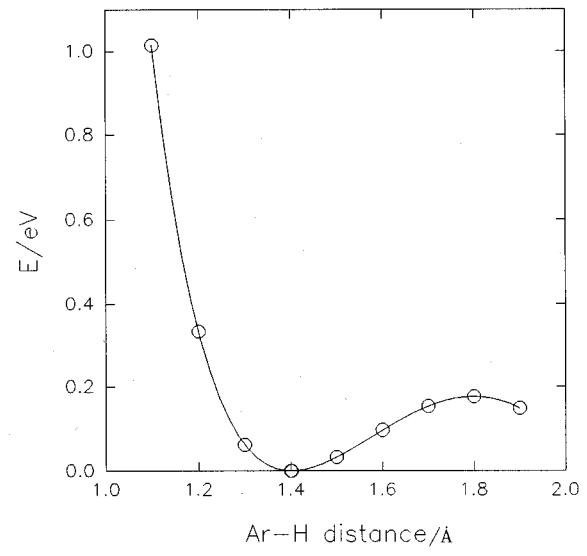

FIG. 8. The UCCSD=Full/6-31G** calculated minimum energy dissociation path of HArF along the Ar–H stretching coordinate.

CONCLUSIONS

In this paper we have shown that the strong infrared absorbers in Kr and Xe matrices, originating from photodissociation of hydrogen halides and subsequent annealing of the matrix, are *neutral charge-transfer species of type* HX^+Y^-. The four compounds observed so far are HXeI, HXeBr, HXeCl, and HKrCl. The identification is based on experiments where HXY species are systematically generated in mixed rare gas matrices, as well as on extensive *ab initio* calculations. Agreement between the stabilities of the calculated HXY species and the observed thermally generated species is excellent. Also, the computed spectra (including intensities) agree with the experimental ones. The high-energy HXY species possess extensive ionic nature in the $HX^+–Y^-$ bond, making these molecules very strong absorbers in the infrared. These species are formed from ionic precursors.

ACKNOWLEDGMENTS

The Center for Scientific Computing (Espoo, Finland) is gratefully acknowledged for providing excellent computing facilities. Dr. Henrik Kunttu is warmly thanked for interesting discussions and for critical reading of the manuscript.

[1] G. Frenking and D. Cremer, in *Structure and Bonding 73, Noble Gas and High Temperature Chemistry*, edited by M. J. Clarke *et al.* (Springer, Berlin, 1990), pp. 17–95.
[2] N. Bartlett, Proc. Chem. Soc. **1962**, 218.
[3] J. H. Holloway and G. J. Schrobilgen, Inorg. Chem. **20**, 3363 (1980).
[4] C. Murchison, S. Reichman, D. Anderson, J. Overend, and F. Schreiner, J. Am. Chem. Soc. **90**, 5690 (1968).
[5] H. Kunttu, J. Seetula, M. Räsänen, and V. A. Apkarian, J. Chem. Phys. **96**, 5630 (1992).
[6] M. Räsänen, J. Seetula, and H. Kunttu, J. Chem. Phys. **98**, 3914 (1993).
[7] H. Kunttu and J. Seetula, Chem. Phys. **189**, 273 (1994).
[8] J. Nieminen, E. Kauppi, J. Lundell, and H. Kunttu, J. Chem. Phys. **98**, 8698 (1993).
[9] J. Nieminen and E. Kauppi, Chem. Phys. Lett. **217**, 31 (1994).
[10] M. E. Fajardo and V. A. Apkarian, J. Chem. Phys. **85**, 5660 (1986).
[11] M. E. Fajardo and V. A. Apkarian, J. Chem. Phys. **89**, 4102 (1988).
[12] M. E. Fajardo and V. A. Apkarian, J. Chem. Phys. **89**, 4124 (1988).
[13] J. C. Evans and G. Y-S. Lo, J. Phys. Chem. **70**, 11 (1966).
[14] J. C. Evans and G. Y-S. Lo, J. Phys. Chem. **71**, 3942 (1967).
[15] I. Last and T. F. George, J. Chem. Phys. **89**, 3071 (1988).
[16] M. J. Frisch, G. W. Trucks, M. Head-Gordon, P. M. W. Gill, M. W. Wong, J. B. Foresman, B. G. Johnson, H. B. Schlegel, M. A. Robb, E. S. Replogle, R. Gomperts, J. L. Andres, K. Raghavachari, J. S. Binkley, C. Gonzalez, R. L. Martin, D. J. Fox, D. J. Defrees, J. Baker, J. J. P. Stewart, and J. A. Pople, GAUSSIAN 92, Revision E.2, Gaussian Inc., Pittsburgh, Pennsylvania, 1992.
[17] C. Møller and M. S. Plesset, Phys. Rev. **46**, 618 (1934).
[18] J. S. Binkley and J. A. Pople, Int. J. Quantum Chem. **9**, 229 (1975).
[19] J. Cizek, Adv. Chem. Phys. **14**, 35 (1969).
[20] G. D. Purvis III and R. J. J. Bartlett, Chem. Phys. **76**, 1910 (1982).
[21] G. E. Scuseria, C. L. Janssen, and H. F. Schäfer III, J. Chem. Phys. **89**, 7382 (1988).
[22] G. E. Scuseria and H. F. Schäfer III, J. Chem. Phys. **90**, 3700 (1989).
[23] P. J. Hay and W. R. Wadt, J. Chem. Phys. **82**, 270 (1985).

[24] W. R. Wadt and P. J. Hay, J. Chem. Phys. **82**, 284 (1985).
[25] P. J. Hay and W. R. Wadt, J. Chem. Phys. **82**, 299 (1985).
[26] L. F. Pacios and P. A. Christiansen, J. Chem. Phys. **82**, 2664 (1985).
[27] M. M. Hurley, L. F. Pacios, P. A. Christiansen, R. B. Ross, and W. C. Ermler, J. Chem. Phys. **84**, 6840 (1986).
[28] L. A. LaJohn, P. A. Christiansen, R. B. Ross, T. Atashroo, and W. C. Ermler, J. Chem. Phys. **87**, 2812 (1987).
[29] N. M. Wallace, J. P. Blaudeau, and R. M. Pitzer, Int. J. Quantum Chem. **40**, 789 (1991).
[30] P. C. Hariharan and J. A. Pople, Theor. Chim. Acta **28**, 213 (1973).
[31] P. C. Hariharan and J. A. Pople, Mol. Phys. **27**, 209 (1974).
[32] M. M. Francl, W. J. Pietro, W. J. Hehre, J. S. Binkley, M. S. Gordon, D. J. DeFrees, and J. A. Pople, J. Chem. Phys. **77**, 3654 (1982).
[33] Z. Huzinaga, *Gaussian Basis Sets for Molecular Calculations* (Elsevier, Amsterdam, 1984).
[34] R. Klein and P. Rosmus, Z. Naturforsch. **39a**, 349 (1984).
[35] Z. Latajka and S. Scheiner, J. Comput. Chem. **8**, 663 (1987).
[36] A. I. Vogel, *A Textbook of Practical Organic Chemistry*, 3rd ed. (Longmans, London, 1962), pp. 180–182.
[37] P. N. Noble and G. C. Pimentel, J. Chem. Phys. **49**, 3165 (1968).
[38] V. E. Bondybey and G. C. Pimentel, J. Chem. Phys. **56**, 3832 (1972).
[39] B. S. Ault, Acc. Chem. Res. **103**, 15 (1982).
[40] D. E. Milligan and M. E. Jacox, J. Chem. Phys. **53**, 2034 (1970).
[41] C. A. Wight, B. S. Ault, and L. Andrews, J. Chem. Phys. **65**, 1244 (1976).
[42] J. Lundell and H. Kunttu, J. Phys. Chem. **96**, 9774 (1992).
[43] J. Lundell, M. Räsänen, and H. Kunttu, J. Mol. Struct. (submitted).
[44] I. Last and T. F. George, J. Chem. Phys. **93**, 8925 (1990).
[45] S. A. Rogers, C. R. Brazier, and P. F. Bernath, J. Chem. Phys. **87**, 159 (1987).
[46] J. W. C. Johns, J. Mol. Spectrosc. **106**, 124 (1984).
[47] P. J. Hay and T. H. Dunning, Jr., J. Chem. Phys. **69**, 2209 (1978).
[48] I. Last and T. F. George, J. Chem. Phys. **87**, 1183 (1987).
[49] R. W. Bickes, Jr., B. Lantzsch, J. P. Tonnies, and K. Walaschewski, J. Chem. Soc. Faraday **55**, 167 (1973).
[50] *CRC-Handbook of Chemistry and Physics*, 72nd ed. (Chemical Rubber, Cleveland, 1991).
[51] J. Tellinghuisen, A. K. Hays, J. M. Hoffman, and G. C. Tisone, J. Chem. Phys. **64**, 2484 (1976).
[52] R. J. Bartlett and J. F. Stanton, in *Reviews in Computational Chemistry*, edited by K. B. Lipkowitz and D. B. Boyd (VCH, New York, 1994), Vol. V.